CLM-P 197

CLM-P 197

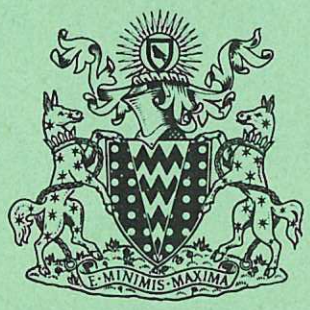

United Kingdom Atomic Energy Authority

RESEARCH GROUP

Preprint

SPECTRA OF HIGHLY-IONIZED NEON AND ARGON IN A PLASMA FOCUS DISCHARGE

N. J. PEACOCK
R. J. SPEER
M. G. HOBBY

Culham Laboratory
Abingdon Berkshire

1969

UNCLASSIFIED
(Approved for Publication)

CLM - P 197

SPECTRA OF HIGHLY-IONIZED NEON AND ARGON IN A PLASMA FOCUS DISCHARGE

by

N.J. Peacock
R.J. Speer*
M.G. Hobby≠

ABSTRACT

Valency electron transitions with up to 4 keV energy in highly-stripped ions are produced in the transient pinch which occurs in a coaxial plasma gun, 'Plasma Focus'.

New or improved wavelengths for transitions in H-like and He-like neon and argon ions are measured and are identified by comparison with Hartree-Fock (HX) calculations of atomic structure, (Cowan; 1966, 1968). Observed wave-lengths of the He-like resonance lines lead to extrapolated values for the ionization potentials of AXVII and NeIX. Inner-shell transitions in less highly-stripped ions are also identified.

* Imperial College, London
≠ Leicester University, Leicester

U.K.A.E.A. Research Group,
Culham Laboratory,
Abingdon,
Berks.

March, 1969

C O N T E N T S

1. INTRODUCTION

In the soft X-ray region of the spectrum Flemberg (1942) was able to excite valency electron transitions in highly-ionized ions using a high-voltage vacuum spark as a source. The shortest wavelength observed by Flemberg was 6·314 Å, ($1s^2\ ^1S_0 - 1s4p\ ^1P_1$, Aℓ XII) which corresponds to 2 keV in excitation energy above the ground level. The vacuum spark, perhaps the most widely used source in the spectroscopy of highly-ionized atoms (Edlén, 1963), has been supplemented in recent years, by many high-temperature plasma devices used in controlled fusion research. These devices have been particularly useful for the inert gases which are difficult to excite in the vacuum spark.

A 30 kJ theta-pinch source (Sawyer et al. 1962, 1963) has produced essentially the same range of energetic transitions as did Flemberg's vacuum spark, (1942). Both groups employed crystal dispersion. At longer wavelengths where grating dispersion is more appropriate the large toroidal pinch ZETA, theta-pinches, and more recently laser-produced plasmas (Fawcett et al. 1964, 1966) have been employed as sources. In these plasma devices the maximum kinetic temperature of the electrons is typically a few hundred eV or less.

The present paper describes the spectra from a pinch device, Plasma Focus, in which the energy-density is considerably higher than in the above sources. The kinetic temperature is more typically 1 keV. As a direct consequence of the high temperature and the high collision rate in this plasma the observed range of optical transitions has been extended to 4 keV. We define optical transitions as unscreened or valency electron transitions. The rare gases, argon and neon, are studied in some detail in the present work, since the excitation of the H- and He-like ions of these atoms illustrates the capability

of the plasma as a spectroscopic source for the study of highly stripped ions in the soft X-ray region. Furthermore, experimental data for the transition energies, term levels and ionization potentials in these ions are notably scarce or absent, (Kelly (1968); Moore (1949)).

In addition to optical transitions the presence of screened or inner-shell transitions (sometimes referred to as X-ray transitions) in less highly ionized ions has been observed in these laboratory plasmas. Such screened transitions appear as satellites to the optical transitions, particularly for increasing nuclear charge in the vacuum spark (Flemberg, 1942) and may even almost completely dominate the line spectrum at a few angstroms (Cohen et al. 1968). Again the existence in solar flares of both optical and screened transitions over the wavelength range 1·3 to 3·1 Å has been demonstrated (Neupert et al, 1967).

The precise identification of these screened transitions has presented a problem since their first observation (Edlén and Tyrén, 1939) and is important for the following reasons. In low resolution measurements (viz. the recent solar observations) the X-ray transitions may be misidentified because of their proximity to optical transitions. Further, a description of the equilibrium conditions in the solar and laboratory plasmas should include an explanation of the intensities of both types of lines. In the Plasma Focus these X-ray transitions are observed to be weak relative to the optical transitions, but on account of the above interest they are listed and in some cases identified by comparison with calculations based on Hartree-Fock-Slater theory. The identification of the optical spectra presents less of a problem.

A source which gives optical spectra of H-like ions in the soft X-ray region allows precise wavelength measurements of unidentified

lines, firstly because the Lyman series can be used as wavelength standards, and secondly because of the potentially high resolution of crystal dispersion. In this work simple crystal and grating spectrometers were used.

2. THE PLASMA SOURCE

The radiation studied in this paper is emitted from a dense, high-temperature plasma which is produced transiently within 2 cm of the end of a coaxial plasma gun, shown schematically with the discharge chamber in Fig.1. The energy source is a 94 μF capacitor bank, which, when operated at 30 kV, delivers a peak current of 1·5 MA into a short circuit with a rise time of 2·45 μsec. The device is operated in a static gas filling of D_2 over a pressure range 0·3 to 3 torr. When an applied voltage in the range 23 kV to 40 kV is switched across the electrodes, the current sheath formed initially across the insulator (Fig.1) is driven towards the 'open' end of the gun. The voltage and pressure are adjusted so that the quasi-radial collapse of the current sheath at the end of the electrodes occurs about peak current, typically 1 MA. This pinch or 'Focus' results in the formation of a filament of hot plasma with a volume of 10^{-2} cm^{-3} which lasts for 10^{-7} seconds. The energy density in the pinch is 5 kJ per cm^{-3}.

The physics of the formation and confinement of the plasma focus has been discussed elsewhere, (Filippov et al., 1962; Agafanov et al., 1968; Mather, 1965) and will not be treated in this paper. Of more direct concern is the spatial reproducibility and emission characteristics of the source.

An X-ray pinhole picture of the compressed plasma filament indicates the hot region of the plasma in Fig.2 and illustrates particularly

that the plasma can deviate off-axis stochastically by ± 1 mm. The record in Fig.2 was taken with seeded heavy gas impurities as it was found empirically that the plasma was spatially more reproducible and of course emitted much more light in these gas-filling conditions.

The soft X-ray emission from the compressed plasma is always accompanied by a high flux of hard ($\gtrsim$ 70 keV) X-rays and between 10^9 and 2×10^{10} neutrons per discharge. The occurence of this large neutron flux, in addition to the discontinuities in the circuit waveforms which result from the large change in circuit impedance due to the implosion, is used as evidence in this work that a high energy-density pinch has been formed.

3. THE EMISSION SPECTRUM

When a heavy gas component is present in the gas-filling the emission in the soft X-ray region is dominated by the spectrum of the highly-stripped ions, the population of which is determined by the transient density and temperature. In the focus the temperature is about 1 keV and the density is of the order of 10^{19} cm^{-3}. With a gas filling typical of that used in this study for the argon lines, 1·1 torr (D_2 + 5% A), T_e the peak electron temperature, has been measured at 1·8 $\pm$ 0·6 keV and the mean density at $1{\cdot}5 \times 10^{19}$ cm^{-3}, (Peacock et al. 1968). A pure gas filling of neon at 0·5 torr was used mainly for generating the Neon ion spectra, and, as discussed in section 6.5, T_e in this case is about 0·4 keV.

In the steady-state approximation the spectrum is readily calculated (House 1964), and Fig.3 shows a plot of the main emission features to be expected in the X-ray region from an argon-doped plasma with plasma parameters approximately those above. It has been pointed

out (Peacock et al. 1968) that in the argon-doped plasma a steady-state population is approached but not achieved. The H-like ion population is suppressed therefore in favour of lower ion stages and the measured ratio of the intensities of the H-like and He-like resonance transitions in argon is less than that shown in Fig.3. The steady-state calculations are however a guide to understanding the observed spectral features.

4. GRATING DISPERSION

For wavelengths longer than the Aℓ k-edge, a 2-metre Rowland circle grating spectrograph (Gabriel, Swain and Waller, 1965) was employed. At a grazing angle of 2^{o}, and with an original glass grating, lightly ruled with 600 lines per mm, the short wavelength limit was about 14 Å, while the use of a gold-coated grating extended the useful wavelength range of the spectrograph to below the k-edge of Aℓ.

An example of the spectrum from the plasma with 1% added Xe using the glass grating, is shown in Fig.4. The step in the continuum at 43·7 Å is due to the carbon absorption edge in the emulsion. With this grating orders higher than the first are weak, so the continuum is not complicated by overlapping orders. Since the first order continuum monotonically increases with decreasing wavelength at least as far as the grating cut-off, this places a lower limit of 440 eV for T_e in this discharge.

The gold-coated, blazed, replica grating which, in contrast to the glass original, showed strong, high-order spectra was employed mainly for investigating the line spectra and in particular the line emission from the Plasma Focus in 0·5 torr neon. A microphotometer trace of the first two orders of the H- and He-like emission neon

ions is shown in Fig.5. The pronounced step in the Lyman continuum of neon at 7·94 Å is due to absorption edge of Aℓ in the 5 micron-thick filter.

The main feature of the emission from H- and He-like argon ions lie well below the Aℓ k-edge, and were dispersed using gratings at shallow grazing angles of about 10 arc minutes to the incident light. The gratings were ruled and etched at N.P.L. to give a high efficiency in the X-ray region, (Franks and Lindsey, 1968). In the first instance, a plane, 300 lines per mm grating was employed to give the spectrum shown in Fig.6 from an argon-doped plasma. The limited resolution is due to the finite aperture of the collimator slits. In the absence of a precise value of α (Fig.6), the dispersion was calculated from the relative positions of the zero order, which appears as a thin line under heavy filtration, and the higher orders. If x_1 and x_2 are the positions of the line feature in the first and second orders in Fig.6, then its wavelength 3·9 ± 0·1 A is given by

$$\lambda = d \frac{x_1 x_2 (x_2 - x_1)}{2R^2 (2x_1 - x_2)} ,$$

where d is the grating spacing and R is the distance from the film to the centre of the grating, Fig.6.

A focusing grating spectrograph with a 5-metre Rowland circle was also designed for this study (Peacock and Speer, 1969), but primarily because of the low photon density along the focusing circle, a useful exposure could only be made after a few discharges when the photographic plate was oriented radially. Fig.7 shows the spectrum from an argon-doped plasma in this focusing configuration and at a 10 arc minute angle of incidence. In this exposure the characteristic radiation from the anode has deliberately not been screened off. The instrument is sufficiently stigmatic to spatially resolve the Cu K lines at

the anode from the argon spectra emitted from the plasma about 2 cm away from the anode. The argon continuum between 7·9 and 15 Å is due to recombination into AXVI, as is calculated for the transmission through an Aℓ filter in Fig.3.

While the resolution of the present grating instruments below 10 Å is much inferior to that which can be achieved using crystal dispersion, this is compensated somewhat by the large energy range (0·1 to 10 keV) covered on one discharge with the 2 and 5 metre instruments. Indeed these spectra (Figs 5 , 6 , 7) extend to shorter wavelengths the range over which optical spectra have previously been recorded using gratings (Tyren, 1938; Gabriel, Swain and Waller, 1965).

5. CRYSTAL DISPERSION RESULTS

The simple de Broglie configuration, in which a crystal is bent convex to the source (Van Rohmann, 1914), is used in this work. The spectrometer is essentially a defocusing instrument where a relatively large spectral range is recorded at the expense of a limited aperture of the crystal for each Bragg reflection. With the intense plasma focus source however, a useful exposure could be obtained with a single discharge. The spectrometer, shown schematically in Fig.8, consists of a wafer of mica wrapped around a cylindrical former three inches in diameter. A film cassette, actually a segment of an outer concentric cylinder, records the Bragg reflections from the convex surface of the mica. The light tangentially incident on the curved crystal serves as a zero wavelength, while along the film plane the dispersion is constant at 0·082 Å/mm. A wavelength range from 0 to 14 Å is recorded on one exposure. A resolution of 0·01 Å was achieved in the third order of the argon lines which lie between 3 Å and 4 Å, and this was determined both by the 'window function' of the mica, 0·002 Å , and

more significantly by the small lateral motions of the source. A displacement of the plasma by 1 mm from the axis during one discharge could explain the 0·02 Å half-intensity width of the lines.

The difficulty of finding standards of wavelength in the X-ray region was overcome by superimposing the first order spectrum of H- and He-like neon with the third order spectrum of argon which lies in the same wavelength region. The wavelengths for neon ions can be accurately calculated (Garcia and Mack, 1965), or can be measured as in the present paper, Table 1. A comparison of the H- and He-like features of both neon and argon are shown in Fig.9.

6. DISCUSSION OF RESULTS

6.1 The Neon Line Spectrum

In order to evaluate neon wavelengths, the data were reduced from comparator readings and densitometer traces of two photographic plates. The first plate displayed only the H-like and He-like neon features, (Fig.5) in the first fifteen orders, the impurity spectrum being excluded with a 5 micron Aℓ filter. In this case, the calculated centroid of the close-spaced doublet $1^2S - 2^2P$ of NeX (Garcia and Mack, 1965) was used as a standard of wavelength throughout the order. The second plate with no Aℓ filter included the strong H-like and He-like lines of carbon, nitrogen and oxygen which were also used as sub-standards of wavelength (Kelly, 1968). Polynomials of degree from quadratic to quintic were fitted to the wavelength standards using the Culham KDF 9 computer and the other wavelengths were evaluated by numerical interpolation on the best-fit dispersion curve. The mean of the wavelengths are shown in Table 1a and have been statistically weighted by the square of the order number. There is no evidence for grating-produced anomalies increasing with order so that wavelength

shifts in the higher orders are discounted. An internal consistency check showed that the higher members $2 < n < 7$ of the NeX Lyman series were predicted to within 0·002 Å of the values calculated by Garcia and Mack, 1965.

6.2 Ionization Potential of Ne IX

It is to be noted that Table 1 lists under Tn, seven term values for n^1P in the neon IX resonance series. Assuming a Ritz formula with $Tn = \frac{RZ^2}{(n^*)^2}$ and $n^* = n - (\mu + \alpha Tn)$, a best fit is found to this series and, extrapolating to $n \to \infty$, an ionization potential is derived.

Using a least squares fit to the observed values, the derived value of ionization potential T_∞ and its 90% confidence limits are 9,645,400 ± 5,300 cm^{-1}, with $\mu = -0{\cdot}004 \pm 0{\cdot}040$ and $\alpha = -0{\cdot}8 \times 10^{-7}$. Following Shenstone and Russell (1932) the best and most sensitive exhibition of an unperturbed term sequence is a plot of the quantum defect of $n^* - n$ against Tn. A set of hyperbolae are produced by choice of T_∞ which, in the limit of T_∞ approaching its true value, reduce to a line of slope α and intercept μ. The plot, Fig.10 shows A, the curve for the derived value of T_∞ while plots B and C show the results of using values 0·05% (0·6 eV) either side of this 'true' T_∞. A displacement of 1×10^6 cm^{-1} has been introduced in these latter curves as a visual aid. The error bars correspond to ± 1 standard deviation of the computed wavelengths. The mean value of the quantum defect is in good agreement with extrapolated results of Edlen (1951), and the ionization potential obtained by the above methods is 1195·84 ± 0·66 eV compared with the extrapolated value of 1195·82 eV, Lotz (1967); $1\ cm^{-1} = 1{\cdot}23981 \times 10^{-4}$ eV is used in this conversion.

It is of interest also to compare the asymptotic value for the quantum defect for the ^{1}P-terms, 0·004, with that measured, ·004, by Flemberg (1942) for the isoelectronic ions Mg XI and Aℓ XII. The difference between the calculated, Lotz (1967), ionization potentials and Flemberg's measured values for these ions is consistently positive, being 0·03% or less for Mg XI and Aℓ XII. In the present work the agreement between experiment and theory is much closer, being 0·002%.

6.3 Neon Satellite Lines

In the microphotometer trace of the first two orders of the Ne X, Ne IX spectrum, Fig.5, several weak lines are observed which do not belong to the resonance series in these ions. Most have been identified as screened transitions in Ne VIII and Ne IX (Table 1a) by comparison with the Hartree-Fock-Slater (H.X) calculations of R.D. Cowan, (Cowan, 1966, 1968). The agreement between experiment and these theoretical calculations has been discussed elsewhere for other configurations in which configuration interaction is not important, (Fawcett, Peacock and Cowan, 1968). For the resonance lines discussed in this paper the agreement is within ·01 A. This leads to good confidence that, provided configuration mixing can be neglected, the inner-shell configurations can be equally well predicted. The configurations responsible for the satellites give rise to a number of multiplets whose structures are not resolvable with the present instruments in low-orders. In Table 1a only the strongest calculated line i.e., the line with the largest weighted oscillator strength, gf, in the multiplet, is listed. It is true, of course, that the experimental intensities will not necessarily be proportional to the gf values, but will depend on the physical conditions of excitation and recombination in the plasma determining the relative ion and excited state populations. For example,

some satellites observed here have somewhat different intensities to those previously reported for a θ-pinch, Sawyer et al. (1962). In the present spectrum the 13·710 Å and 13·654 Å lines due to Ne VIII, Table 1a, are of equal intensity. In the θ-pinch, on the other hand, the 13·710 Å line is absent and a line at 13·84 Å which coincides with the strongest calculated line in Ne VII, $1s^2 2s^2 - 1s2s^2 2p$, is present.

Interest in the group of inner-shell transitions, $1s^2 n\ell - 1s2pn\ell$ with n = 2, stems from the possibility that they may account for a solar line at 22·09 Å which is surprisingly strong relative to the O VII resonance lines (Jones, Freeman and Wilson, 1968). In the spectrum of plasma focus typically two lines of equal intensity are observed at 22·014 Å and 22·121 Å, close to the wavelength of the solar line. These laboratory lines are O VI , isoelectronic with 13·654 Å and 13·710 Å in Ne VIII and with 3·983 Å and 3·987 Å in A XVI and due to the transitions $1s^2 2s - 1s2s2p$ and $1s^2 2p - 1s2p^2$ (Table 1). From the calculated positions of these multiplets with the largest gf values we would tentatively assign the upper terms $1s2p^2\ ^2D$ to the longer wavelength and a blend of $1s2p^2\ ^2P$ and $1s2s2p\ ^2P$ to the shorter of the two wavelengths, Table 1. There is no doubt that these configurations are responsible for the lines since higher members (n = 3,4) of the series are also observed (Table 1).

Because of the overlap in wavelength of the calculated multiplets it is not possible in this paper to give a more detailed identification of these inner-shell lines. However, in a current publication in which configuration mixing is taken into account, Gabriel and Jordan have been able to assign multiplets to this isoelectronic sequence for ions up to Aℓ XI and in addition to identify the 22·09 Å solar line, (Gabriel and Jordan, 1969). The present assignment of configurations

is in agreement with the detailed identifications of Gabriel and Jordan.

6.4 Intercombination Lines in Ne IX

Under certain conditions of plasma density and temperature when it is evident that the lines are optically thin and that recombination from the continuum does not affect the population of the $n=2$ levels, the ratio R of the resonance line $1s^2\ {}^1S_0 - 1s^2\ 2p\ {}^1P_1$ to the intercombination line $1s^2\ {}^1S_0 - 1s2p\ {}^3P_1$ in the He-like ions is only weakly dependent on temperature and gives a direct measure of N_e, the electron density, (Kunze, Gabriel and Griem, 1968). This method of measuring density is independent of the spectrograph and plate calibration and of spatial variations in the source, since the lines in question lie at about the same wavelength and arise from the same ion. Because of the small dimensions, (0·1 cm) of the hot plasma, the optical opacity is not thought to give rise to serious error, nor indeed is recombination into the $n=2$ level considered to be serious at T_e = 400 eV (viz. section 6.5) in the neon plasma. The experimental value of R tends to a limiting value of 7·5 with increasing order number when the densities, D, of the lines lie within the linear range of the Q2 emulsion ($0{\cdot}1 < D < 0{\cdot}3$). A comparison with the theoretical model yields a value $N_e = 5{\cdot}7 \times 10^{18}$ cm^{-3} for a gas filling of 0·5 torr neon, the maximum error being a factor of two. This evaluation of density is within a factor of three of the density already estimated from the absolute photon flux in somewhat different gas conditions, Peacock et al, (1968).

6.5 Neon Continua

The intensity of the Lyman and He-like continua can be appreciated from the height of the absorption step at 7·94 Å due to the 5μ Aℓ

filter (Fig.6). The electron temperature can be derived directly from the product of the exponent $e^{-h\nu/kT}$ in the continuum intensity and the transmission of the Aℓ filter. The spectrograph response is taken to be constant over the narrow wavelength region between the absorption edge and the Lyman series limit at 9·102 Å. It follows directly from the wavelength at which the observed continuum reaches a flat maximum at 8·67 Å, that the electron temperature, T_e, is 400 (± 100) eV.

Alternatively, T_e can be calculated from the height of the free-bound discontinuity at the Ne X, Ne IX series limits, McWhirter (1965). This method has the advantage that it makes in principle, no recourse to assumptions of constant spectrograph response with wavelength. To a good approximation the photon-flux step-ratio R at the Lyman series limit of NeX is given by

$$R' = 2{\cdot}6 \frac{g_{fb}(\text{Ne XI})}{g_{fb}(\text{Ne X})} \cdot \frac{N(\text{Ne XI})}{N(\text{Ne X})} \exp \cdot \left[\frac{\psi(\text{Ne X}) - \psi(\text{Ne IX})}{kT} \right]$$

where g_{fb} is the free-bound gaunt factor and the remaining factors are the population ratio of Ne XI/Ne X and an exponent involving the ionization potentials ψ and the temperature. If in the first instance we assume a steady-state relative ion population such as that tabulated by House (1964), a graphical solution of the above equation with $R' = 1{\cdot}3$, gives $T_e = 300$ eV ± 50 eV. The assumption of an ion population described by a balance between collisional ionization and collisional radiative recombination is well-justified for ionization potentials greater than 1 keV and a density of the order of 10^{19} cm^{-3}.

The above agreement between the Lyman-step measurement and the continuum shape temperature is to be taken as evidence that with a gas filling of 0·5 for neon the plasma has a substantially steady-state ion population. The application of the Lyman continuum in the

measurement of T_e has not hitherto been possible in the soft X-ray region, and is a direct consequence of the high value of the product $N_e\tau$ where τ is the plasma confinement time, and the approach to steady-state conditions in the Plasma Focus.

6.6 The Argon Line Spectrum

The wavelengths of the de Broglie spectrum shown in Fig.9 were reduced using the same techniques described in Section 6.1. The H-like and He-like neon lines in the first order and Lyman-α of A XVIII in the third order were used as standards of wavelength. The wavelengths for the Ne IX optical transitions reduced from the crystal data agreed with the wavelengths, Table 1a, reduced from the grating data within the experimental errors shown. The grating wavelengths, Table 1a and the crystal wavelengths, Table 1b, are thus self-consistent. The first five members of the He-like argon resonance series are observed and their measured wavelengths are listed in Table 1b with their absolute term values. It is to be noted that the measure of agreement between the experimental and calculated wavelengths in A XVII and A XVIII, Table 1b, is within 0·004 Å.

Only the first member of the Lyman series was observed, however, and on comparison of the line intensities in Fig.9 with that calculated in Fig.3 for a gas filling of 1·1 torr (D_2 + 5% A), it is apparent that the Lyman-α line is relatively less intense than a steady-state would allow, in distinction to the neon plasma (see Section 6.5).

6.7 Argon Satellite Lines

By comparison with the calculations the configurations responsible for some of the satellite lines have been identified: again the calculated lines in these multiplets with the highest values of gf

have been listed, (Table 1b). Three members of the inner shell series $1s^2 2s - 1s2snp$, $1s^2 2p - 1s2pnp$, $(n \geq 2)$, in Li-like ions are observed and are stronger in the argon spectrum than in the neon (Fig.9). The identifications with a question mark on Table 1b are uncertain to the extent that the limited resolution would allow one or two more or less screening electrons in the configuration.

6.8 Intercombination Lines in A XVII

In the low-density limit, when depletion of the triplet and singlet $n=2$ level populations in He-like ions is by spontaneous decay to the ground state, the singlet/triplet intensity ratio R approximates simply to the ratio of the excitation rates from the ground state. This is independent of ion charge and has a value of 1·8, (Kunze, Gabriel and Griem, 1968). This situation obtains in this plasma condition when the measured plasma parameters, Peacock et al (1968), are $N_e \simeq 1{\cdot}5 \times 10^{19}$ cm^{-3} and $T_e = 1{\cdot}6$ keV. R is measured from the de Broglie spectrum to be $1{\cdot}65 \pm 0{\cdot}4$, in good agreement with theory.

6.9 Ionization Potentials of A XVII

Using the procedures and limits of Section 6.2 the ionization potential of A XVII was found to be 33,200,000 ± 70,000 cm^{-1} or 4116 (± 9 eV within the 90% confidence limits), compared with an extrapolated value of 4121 eV, Lotz (1967). The derived value of μ is $- 0{\cdot}04 \pm 0{\cdot}05$. This error limit in the ionization potential and in the quantum defect, which is larger in argon than in neon, is due to the breadth of the lines and therefore the uncertainty in their wavelengths in the crystal spectrum.

7. SUMMARY

Valency electron transitions with up to 4 keV energy have been measured in the Plasma Focus device when the 'carrier' gas, D_2, is seeded with a few percent of argon. This confirms in order of magnitude a 1 keV temperature in the plasma. As a consequence to the high temperature and to the high value of the product $n_e\tau$ (n_e is the electron density and τ the ion confinement time) it should be possible to extend the study of optical transitions even further into the X-ray region by introducing higher z elements into the plasma.

The intensity of the source when run in the above gas condition is sufficient to give useful records in the X-ray region from a single discharge, despite the use of small aperture, rather inefficient instruments. Moreover, optical transition intensities are intense relative to screened transitions and this is in contrast to other sources such as the high-voltage vacuum spark.

When the focus is fired in 0·5 torr neon, the plasma temperature is of the order of 400 eV and the Lyman continuum with known intensity distribution extends well below 10 Å.

The Ne IX and A XVII resonance lines are identified and a Ritz extrapolation of the principal quantum number leads to experimental values of the ionization potentials of these ions. Weaker satellite lines in lower ionization stages have been identified by comparison with Hartree-Fock-Slater theory. These identifications will allow isoelectronic extrapolation to higher ions, e.g., Ca, Fe and Ni which are important in the solar flare spectrum. The agreement between the Hartree-Fock (HX) calculations and the present experimental wavelengths suggests that these tranisitions in the above higher z elements can be calculated to better than 0·01 Å, and to about 0·001 Å for the resonance lines.

ACKNOWLEDGEMENTS

The authors would like to thank N. Sanitt, R. Mahon and S. Budd for their help in the analysis of the spectra. The Hartree-Fock (HX) calculations which are much more extensive than is apparent from this paper were generously contributed by Dr R.D. Cowan of the Los Alamos Scientific Laboratory. The choice of the de Broglie configuration for dispersion of the emission in the X-ray region was suggested to us several years ago by Dr R.D. Deslattes of N.B.S., Washington, D.C. - it only awaited a sufficiently intense source to make use of his suggestion. The co-operation of Dr A. Franks, N.P.L. in ruling the X-ray gratings is also gratefully acknowledged.

REFERENCES

AGAFANOV, V.I. et al. (1968) 3rd Int. Conf. on Plasma Physics and Nuclear Fusion, Novosibirsk. Paper CN-24/G-2. to be published (1969) I.A.E.A. Vienna.

COWAN, R.D. (1966) J. Opt. Soc. Am., 56, p.1416.

COWAN, R.D. (1968) Private communication.

COHEN, L., FELDMAN, U., SWARTZ, M. and UNDERWOOD, J.H. (1968), J. Opt. Soc. Am., 58, pp.843-846.

EDLÉN, B. (1951), Arkiv. fu. Fysik., 4, pp.441-453.

EDLÉN, B. and TYRÉN, F. (1939) Nature, 143, p.940.

EDLÉN, B. (1963) Reports on Progress in Physics, vol.XXVI, pp.181-212.

FAWCETT, B.C., GABRIEL, A.H., JONES, B.B. and PEACOCK, N.J. (1964) Proc. Phys. Soc., 84, pp.257-262.

FAWCETT, B.C., GABRIEL, A.H., IRONS, F.E., PEACOCK, N.J. and SAUNDERS, P.A.H. (1966) Proc. Phys. Soc., 88, pp.1051-1053.

FAWCETT, B.C., PEACOCK, N.J. and COWAN, R.D. (1968) Proc. Phys. Soc., 2, 1, pp.295-306.

FILIPPOV, N.V., FILIPPOVA, T.I. and VINOGRADOV, V.P. (1962) Nuclear Fusion Suppl., pt.2, p .577-587.

FLEMBERG, H. (1942) Ark. Nat. Astr. O. Fys., 28, A, 18, pp.1-47.

FRANKS, A. and LINDSEY, K. (1968) J. Sci. Instrum., Series 2, 1, p.144.

GABRIEL, A.H., SWAIN, J.R. and WALLER, W.A. (1965) J. Sci. Instrum., 42, pp.94-97.

GABRIEL, A.H. and JORDAN, C. (1969) Submitted to Nature.

GARCIA, J.D. and MACK, J.E. (1965) J. Opt. Soc. Am., 55, pp.654-685.

HOUSE, L.L. (1964) Astrophys. J. Suppl.VIII, 81, pp.307-328.

HOUSE, L.L. (1968) Submitted to Astrophys. J. Suppl.

JONES, B.B., FREEMAN, F.F. and WILSON, R. (1968) Nature, 219, p.252.

KELLY, R.L. (1968) 'Atomic Emission Lines below 2000 Å , Hydrogen through Argon'. N.R.L. Report 6648.

KUNZE, H.J., GABRIEL, A.H. and GRIEM, H.R. (1968) Phys. Fluids, 11 pp.662-668.

LOTZ, W. (1967) J. Opt. Soc. Am., 57, pp.873-878.

MATHER, J.W. (1965) Proc. Conf. Plasma Physics and Controlled Nuclear Fusion, Culham. (Vienna, I.A.E.A.) vol.II, pp.389-404.

MOORE, C.E. (1949) Atomic Energy Levels (Washington, D.C.: National Bureau of Standards) N.B.S. Circular 467.

McWHIRTER, R.W.P. (1965) In 'Plasma Diagnostic Techniques' (Huddlestone R.H. and Leonard, L.L. eds.) (New York: Academic Press) Ch.5

NEUPERT, W.M., GATES, W., SWARTZ, M. and YOUNG, R. (1967) Astrophys. J., 149, pp.L79-83.

PEACOCK, N.J., WILCOCK, P.D., SPEER, R.J. and MORGAN, P.D. (1968) Paper CN-24/G-4, 3rd Int. Conf. on Plasma Physics and Nuclear Fusion. Proceedings to be published by I.A.E.A. Vienna.

PEACOCK, N.J. and SPEER, R.J. (1969) To be submitted to J. Sci. Instrum.

ROHMANN, H. Van. (1914) Zeit. fur Phys., 15, pp.510-512.

SAWYER, G.A., JAHODA, F.C., RIBE, F.L. and STRATTON, T.F. (1962) J. Quant. Spectrosc. Rad. Transfer, 2, pp.467-475.

SAWYER, G.A., BEARDEN, A.J., HENINS, I., JAHODA, F.C. and RIBE, F.L. (1963) Phys. Rev., 131, pp.1891-7.

SHENSTONE, A.G. and RUSSELL, H.N. (1932) Phys. Rev., 39, p.415

TYREN, F. (1938) Zeit. fur Phys., 111, p.314

TABLE 1(a)

NEON

	Ion	λ, Å	Intensity	±δλ, Å	T_n cm^{-1}	Identification	Theory	Prior Work
Unscreened transitions	NeIX	13.447	100	.002	2,208,800	$1s^2\ ^1S_0 - 1s2p\ ^1P_1$	13.456*	13.45+
	NeIX	11.544	57	.002	982,900	$1s^2\ ^1S_0 - 1s3p\ ^1P_1$	11.545*	11.54+
	NeIX	11.001	35	.002	555,300	$1s^2\ ^1S_0 - 1s4p\ ^1P_1$	10.998*	
	NeIX	10.765	23	.002	356,000	$1s^2\ ^1S_0 - 1s5p\ ^1P_1$		10.76+
	NeIX	10.646	12	.003	252,200	$1s^2\ ^1S_0 - 1s6p\ ^1P_1$		
	NeIX	10.565	7	.006	180,200	$1s^2\ ^1S_0 - 1s7p\ ^1P_1$		
	NeIX	10.513	5	.010	133,400	$1s^2\ ^1S_0 - 1s8p\ ^1P_1$		
		Ionization limit			9,645,400 ± 5300		9,646,799 cm^{-1}	po
	NeIX	13.549	15	.004		$1s^2\ ^1S_0 - 1s2p^3P_1$	13.554*	13.55
	NeIX	78.300	10	.005		$1s2p^3P - 1s3d^3D$		
	NeIX	58.468	10	.005		$1s2p^3P - 1s4d^3D$		
Screened transitions	NeIX	12.303	5	.005		$1s2s^3S_1 - 2s2p^3P_2$	12.303*	
		12.355	5	.005		$1s2p^1P_1 - 2p^2\ ^1D_2$	12.345*	
	NeVIII	13.710	7	.005		$1s^22p - 1s2p^2$	13.709* ($^2P_{3/2}$-$^2D_{5/2}$)*	
	NeVIII	13.654	7	.005	Blend	$1s^22s - 1s2s2p$	13.662* ($^2S_{1/2}$-$^2P_{3/2}$)*	13.66
						$1s^22p - 1s2p^2$	13.682* ($^2P_{3/2}$-$^2P_{3/2}$)*	
	NeVIII	11.905	<5	.005	Blend	$1s^22s - 1s2s3p$	11.885*	
						$1s^22p - 1s2p3p$	11.941*	
		12.825	<5	.004				
		12.535	<5	.005				
		11.392	<5	.005				

* R.D. Cowan - Private Communication (highest gf in multiplets)

\+ Sawyer et al (1963)

po Predicted, Lotz (1967)

TABLE 1(b)

ARGON

	Ion	λ, Å (observed)	Intensity	±δλ, Å	$T_n cm^{-1}$	Identification	Theory	Prior Work
Unscreened Transitions	AXVII	3.944	100	.002	7,845,000	$1s^2\ {}^1S_0 - 1s2p\ {}^1P_1$	3.948*	
	AXVII	3.362	19	.003	3,455,800	$1s^2\ {}^1S_0 - 1s3p\ {}^1P_1$	3.364*	
	AXVII	3.198	13	.005	1,930,400	$1s^2\ {}^1S_0 - 1s4p\ {}^1P_1$	3.198*	
	AXVII	3.137	0	.007	1,322,400	$1s^2\ {}^1S_0 - 1s5p\ {}^1P_1$		
	AXVII	3.09	0	.01	837,500	$1s^2\ {}^1S_0 - 1s6p\ {}^1P_1$		
		Ionization limit			33,200,000 ± 70,000		33,260,694 cm^{-1}	P^o
	AXVII	3.963	55	.002		$1s^2\ {}^1S_0 - 1s3p\ {}^3P_1$	3.966*	
	AXVIII	3.730	13	.003		$1s^2S_{1/2} - 2p\ {}^2P_{3/2}$	3.731+	
	AXVI	3.989	26	.003		$1s^22p - 1s2p^2$	$3.991^*\ ({}^2P_{3/2} - {}^2D_{5/2})^*$	
	AXVI	3.984	26	.003	Blend	$1s^22s - 1s2s2p$	$3.980^*\ ({}^2S_{1/2} - {}^2P_{3/2})^*$	
						$1s^22p - 1s2p^2$	$3.984^*\ ({}^2P_{3/2} - {}^2P_{3/2})^*$	
	AXVI	3.425	15	.005		$1s^22p - 1s2p3p$	3.427*	
	AXVI	3.41	0	.01		$1s^22s - 1s2s3p$	3.417*	
	AXVI	3.264	0	.006		$1s^22p - 1s2p4p$	3.270*	
	AXVI	3.25	0	.01		$1s^22s - 1s2s4p$	3.259*	
Screened Transitions	AXV	4.010	7	.005		$1s^22s^2 - 1s2s^22p$	4.009*	
	AXV	3.45	0	.01		$1s^22s^2 - 1s2s^23p$	3.461*	
	AXV	3.33	0	.015		$?1s^22s^2 - 1s2s^24p$	3.314*	
		3.29	0	.015				
	?AXIV	4.07	5	.01		$?1s^22s^22p - 1s2s^22p^2$	4.050*	
	?AXII	4.12	5	.01		$?1s^22s^22p - 1s2s^22p^5$	4.119^o	
		4.19	0	.01				
	?AII	3.87	5	.01		$?1s^2,-,3p^5 - 1s,-,3p^6$	3.882*	
	?AIX	3.80	5	.01		$?1s^22s^22p^6 - 1s2s^22p^23p$	3.825*	

^{o} House (1968)

\+ Predicedted Garcia & Mack, 1965

* R.D. Cowan - private communication (highest gf in multiplet)

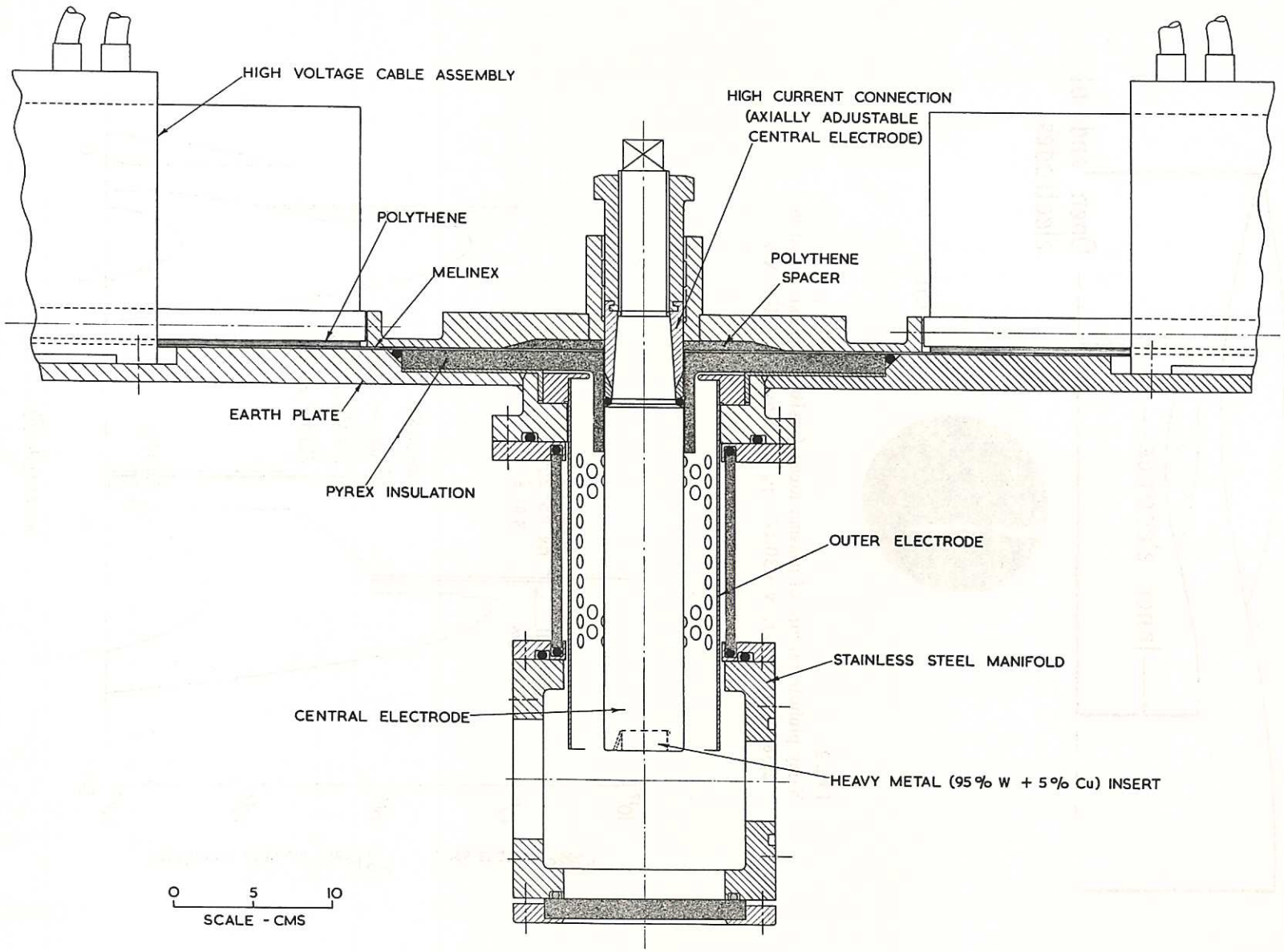

Fig. 1 Schematic diagram of Plasma Focus apparatus (CLM-P197)

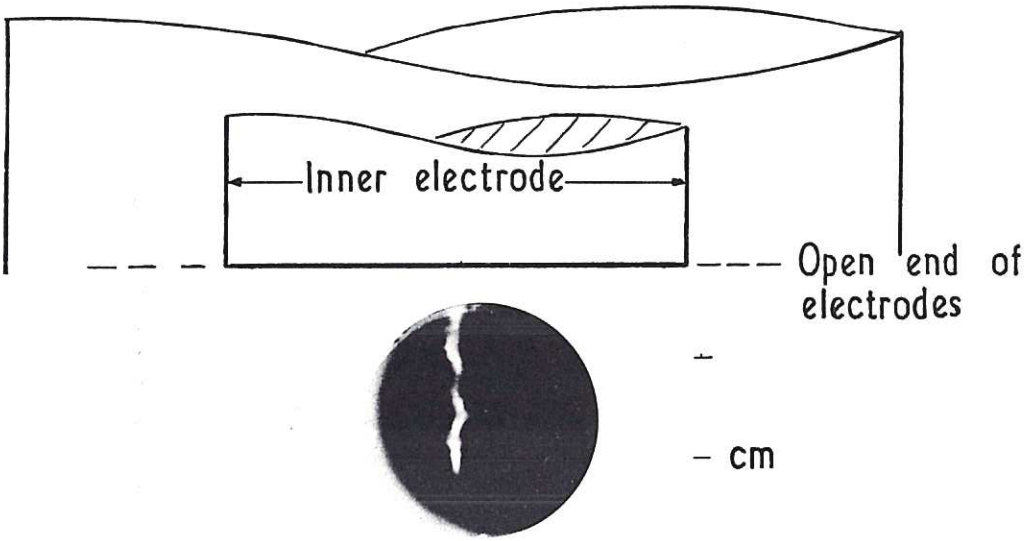

Fig. 2 (CLM-P 197)
X-ray pinhole picture of plasma focus (visible light screened by 2.68 mg/cm² Aℓ); v = 30 kV. p_0 = 1.2 torr (D_2 + 10% Xe)

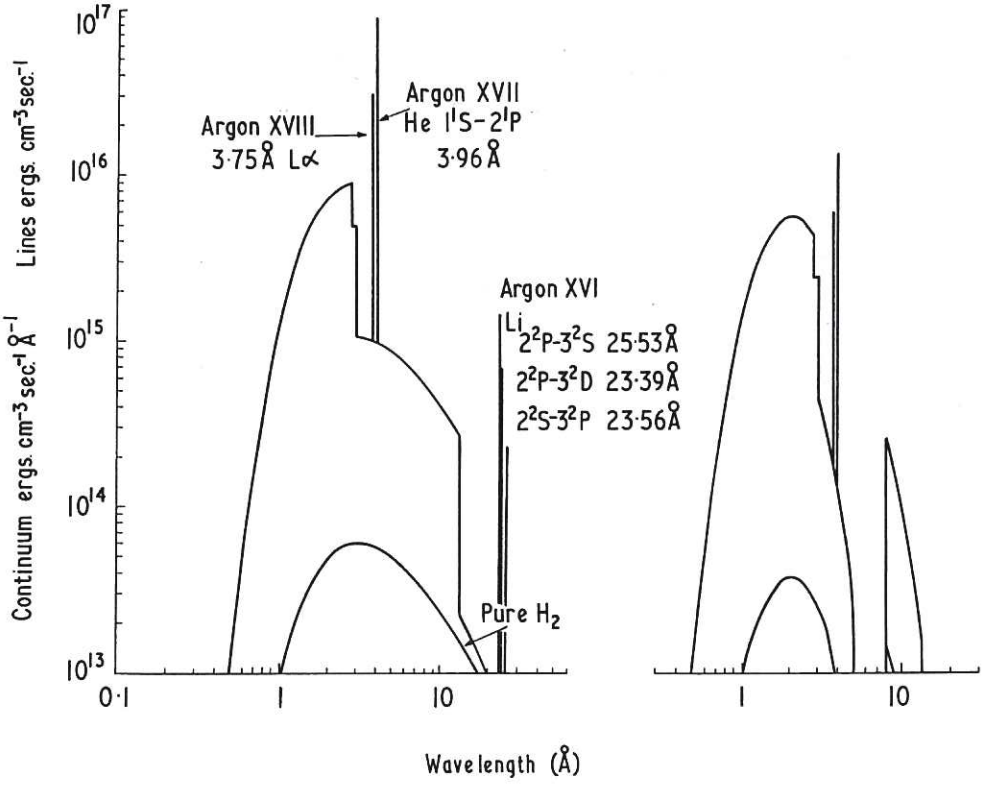

Fig. 3 (CLM-P 197)
Calculated emission spectrum from Plasma Focus (D_2 + 3% Argon)
$N_e = 1.5 \times 10^{19}$ cm^{-3}, T_e = 2 keV

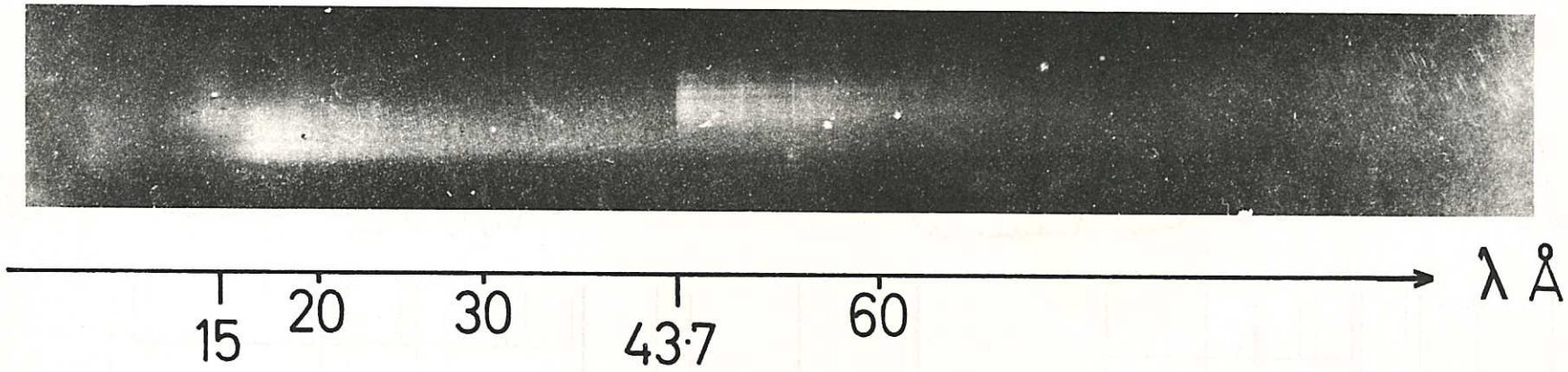

Fig. 4 (CLM-P 197)
Grazing incidence spectrum of Plasma Focus (1.3 torr, D_2 + 1% Xe)

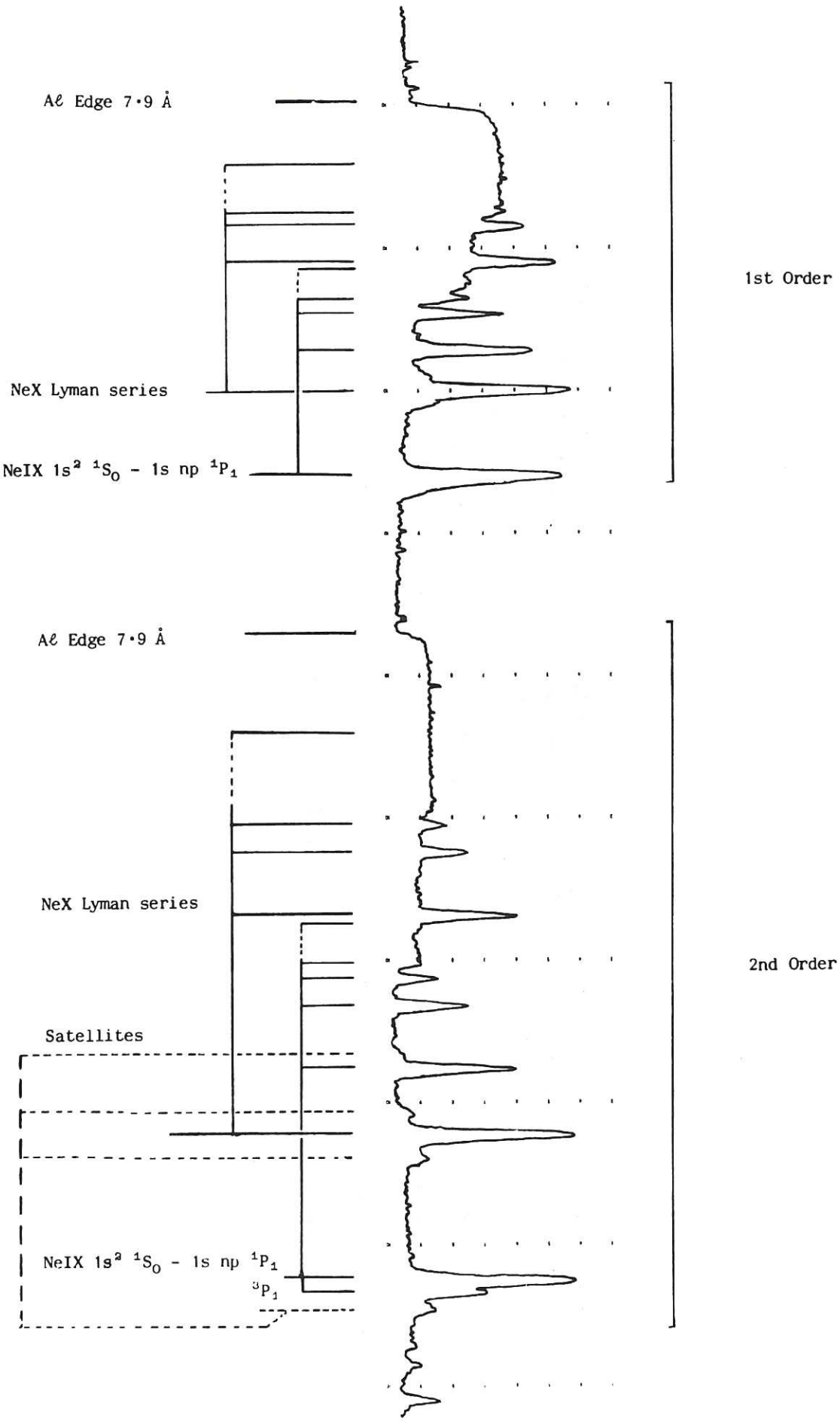

Fig. 5 (CLM-P197)

2° Grazing incidence spectrum of Plasma Focus in 0.5 torr neon: 5 micron filter of Aℓ transmits only Ne IX and Ne X: 1st and 2nd order spectra shown

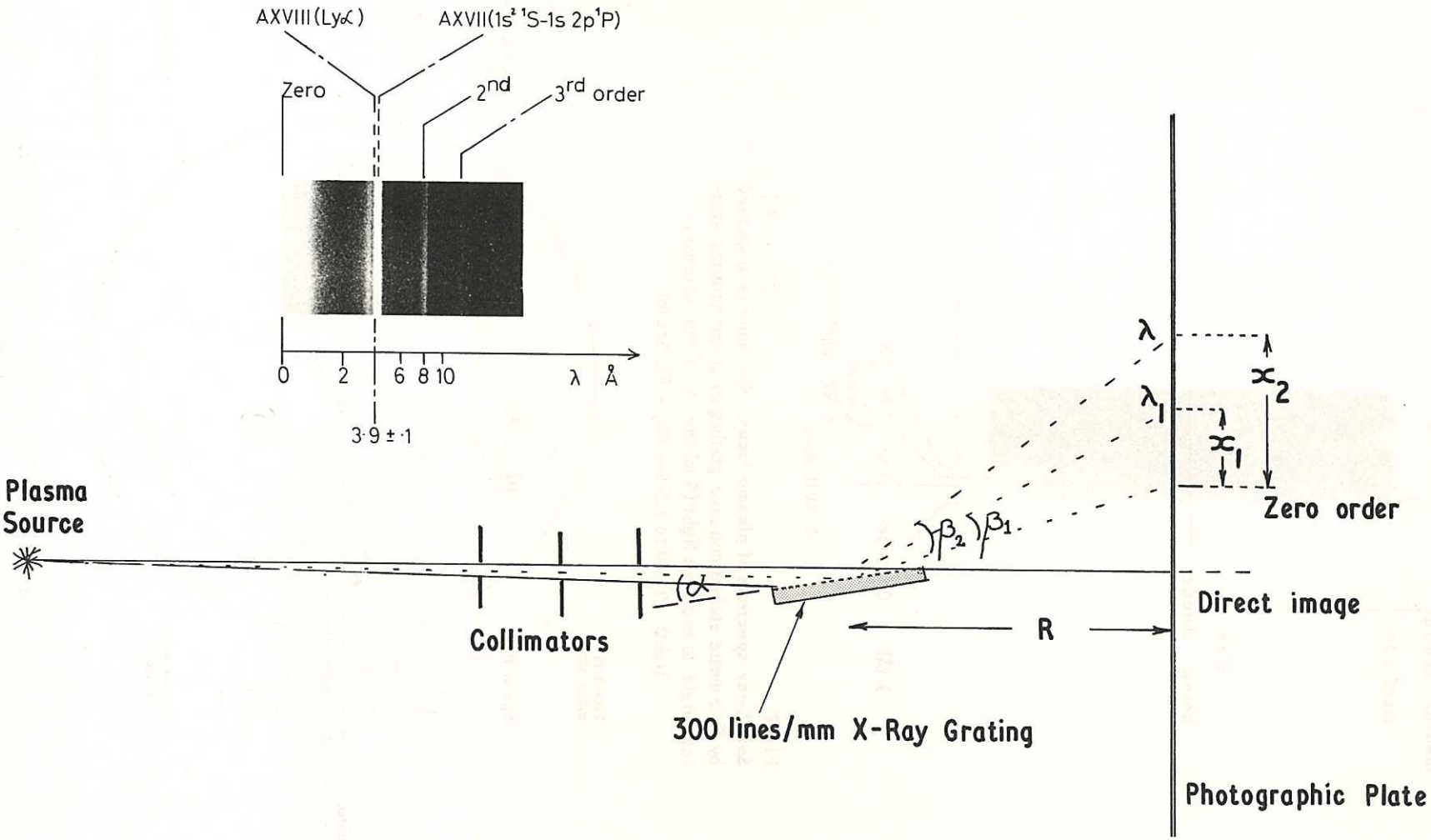

Fig. 6

(CLM-P 197)

Soft X-ray spectrum of plasma focus taken with plane, etched grating at 10 arc minutes, grazing angle and 2 arc minutes collimation of source. Pressure filling 1.3 torr D_2 + 10% Argon

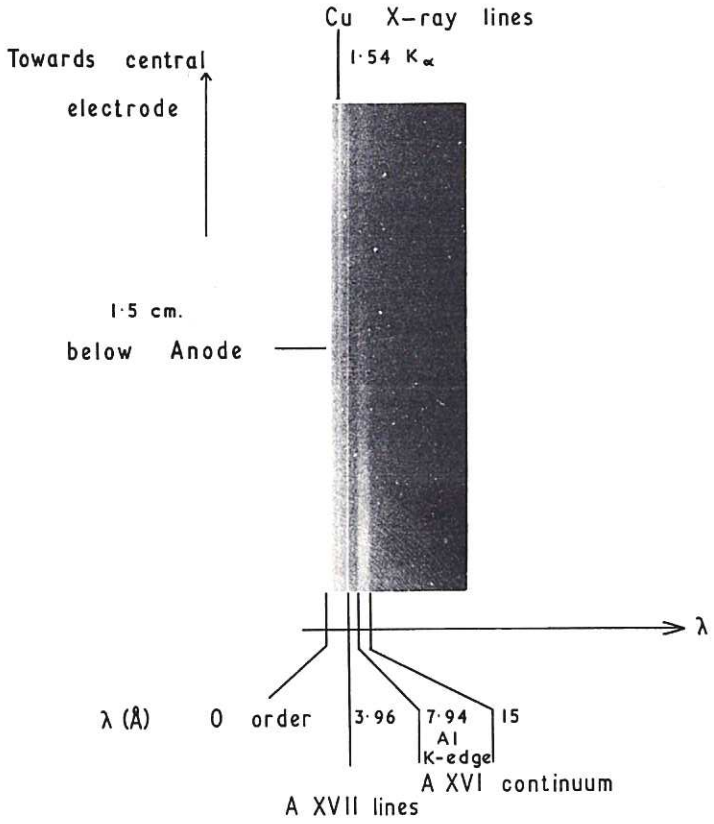

Fig. 7 (CLM-P197)

Soft X-ray spectrum of plasma focus. Spectrum is dispersed by five metre etched concave grating at 10 arc minutes grazing angle to incident light (5 micron Aℓ filter screening light) Pressure 1.5 torr (D_2 + 5% Argon)

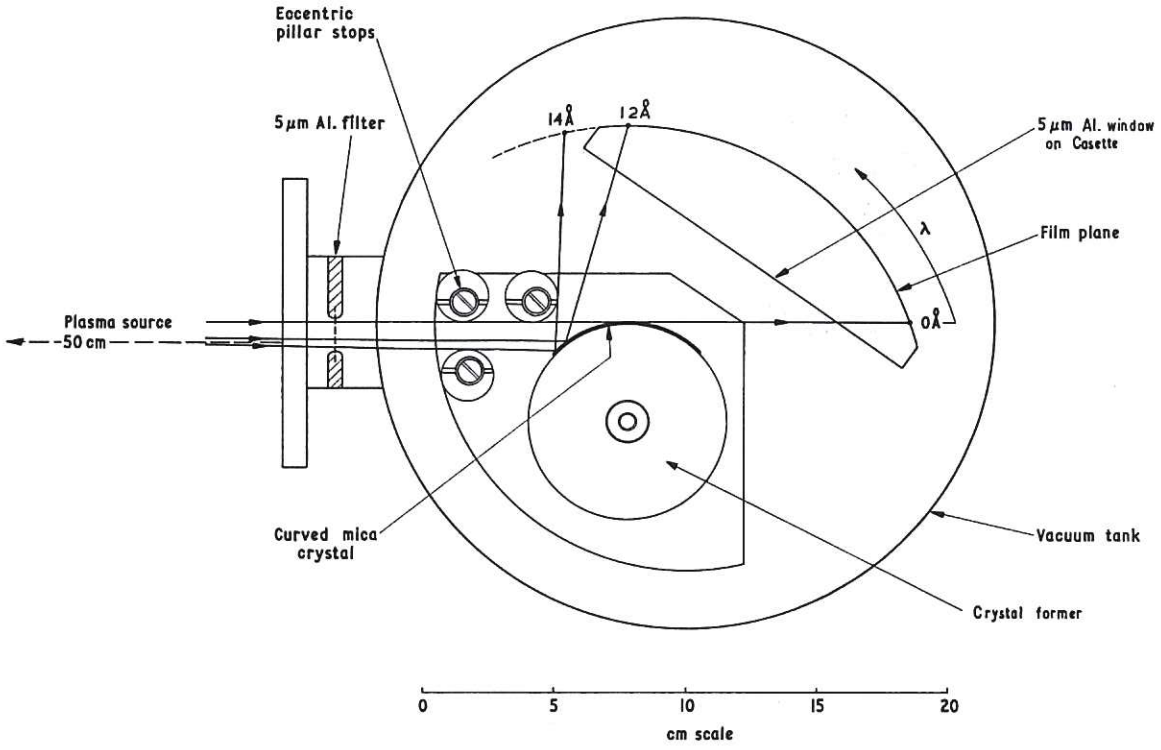

Fig. 8 de Broglie mica crystal spectrometer (CLM-P197)

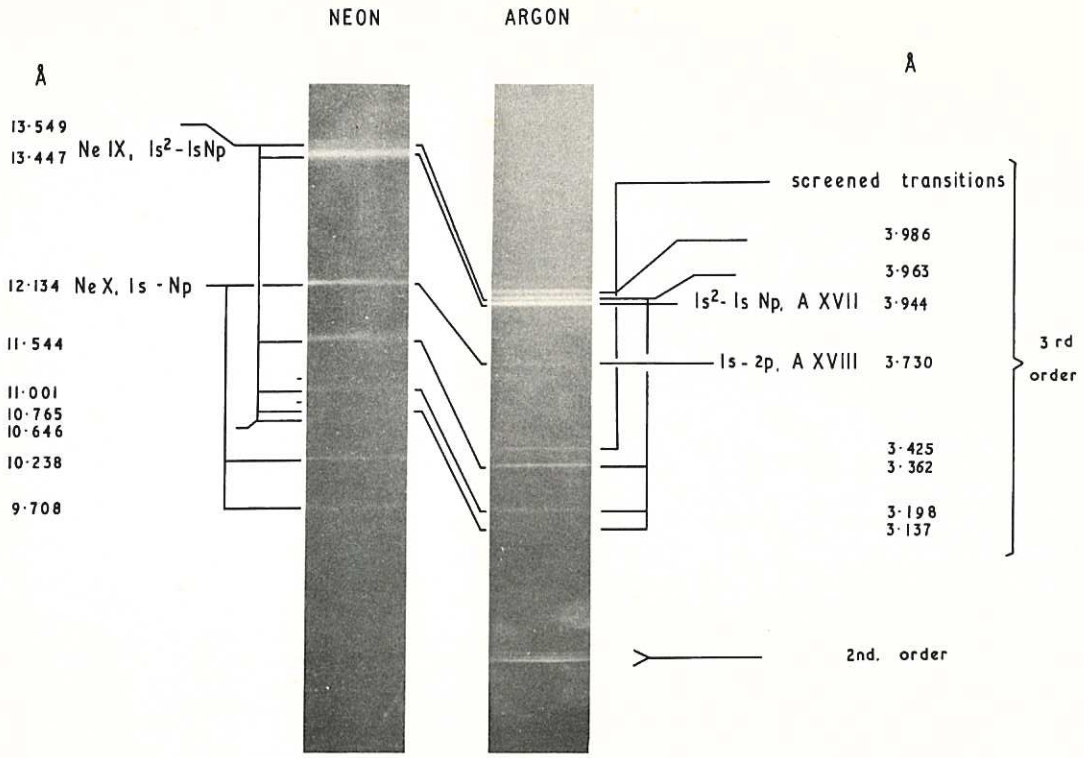

Fig. 9 (CLM-P197)

Curved mica spectrograms of Plasma Focus showing H 1- and He 1-like spectra of neon and argon in wavelength region 3 to 14 angstroms

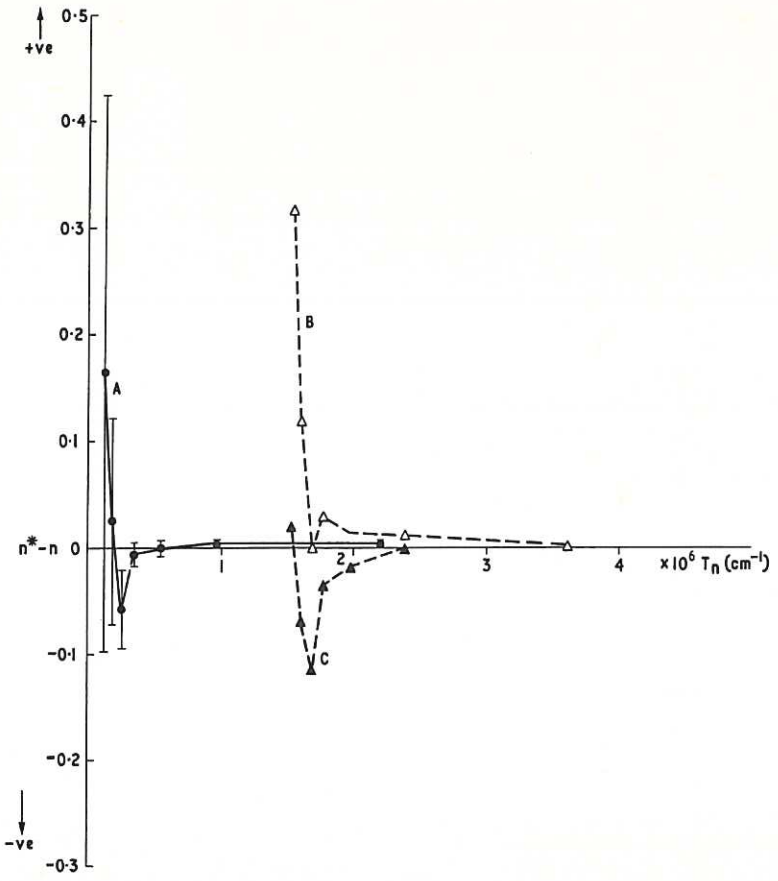

Fig. 10 (CLM-P197)

Quantum defect (n* - n) for n^1P terms in NeIX